Accepted Manuscript

Cytotoxic labdane diterpenes and bisflavonoid atropisomers from leaves of *Araucaria bidwillii*

Sherif S. Ebada, Aya N. Talaat, Rola M. Labib, Attila Mándi, Tibor Kurtán, Werner E.G. Müller, AbdelNasser Singab, Peter Proksch

PII: S0040-4020(17)30387-3

DOI: 10.1016/j.tet.2017.04.015

Reference: TET 28616

To appear in: *Tetrahedron*

Received Date: 26 February 2017

Revised Date: 25 March 2017

Accepted Date: 10 April 2017

Please cite this article as: Ebada SS, Talaat AN, Labib RM, Mándi A, Kurtán T, Müller WEG, Singab A, Proksch P, Cytotoxic labdane diterpenes and bisflavonoid atropisomers from leaves of *Araucaria bidwillii*, *Tetrahedron* (2017), doi: 10.1016/j.tet.2017.04.015.

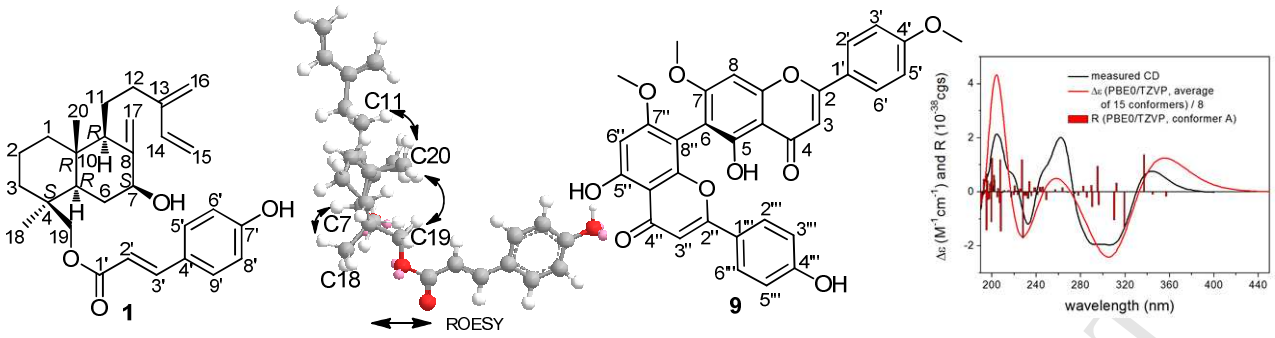

Cytotoxic Labdane Diterpenes and Bisflavonoid Atropisomers from Leaves of *Araucaria bidwillii*

Sherif S. Ebada[a,b], Aya N. Talaat[b], Rola M. Labib[b], Attila Mándi[c], Tibor Kurtán[c], Werner E.G. Müller[d], AbdelNasser Singab[b], Peter Proksch[a]

[a] Institute of Pharmaceutical Biology and Biotechnology, Heinrich-Heine Universität Düsseldorf, Universitätsstrasse 1, 40225 Düsseldorf, Germany

[b] Department of Pharmacognosy, Faculty of Pharmacy, Ain-Shams University, Abbasia, 11566 Cairo, Egypt

[c] Department of Organic Chemistry, University of Debrecen, P. O. Box 400, H-4002 Debrecen, Hungary

[d] Institut für Physiologische Chemie, Universitätsmedizin der Johannes Gutenberg-Universität Mainz, Duesbergweg 6, 55128 Mainz, Germany

*Corresponding authors. Tel.: +49 211 81 14163; Fax: +49 211 81 11923; e-mail addresses: sherif_elsayed@pharma.asu.edu.eg (S.S. Ebada), proksch@uni-duesseldorf.de (P. Proksch).

Abstract

Chemical investigation of a methanolic extract of leaves from *Araucaria bidwillii* (Araucariaceae) from Egypt afforded four new labdane diterpenoidal metabolites (**1**-**4**) together with one known diterpene, 7-oxocallitrisic acid (**5**), two triterpenoidal metabolites, 2-*O*-acetyl-11-keto-boswellic acid (**6**) and *β*-sitosterol-3-*O*-glucopyranoside (**7**), phloretic acid (**8**), and two methylated bisflavonoids, agathisflavone-4',7,7"-trimethyl ether (**9**) and cupressuflavone-4',7,7"-trimethyl ether (**10**). The new metabolites **1**–**4** were unambiguously identified by applying extensive 1D and 2D NMR spectroscopic studies as well as HRESIMS. The relative and absolute configurations of **1**–**4** were determined using ROESY and the modified Mosher's method, respectively. All isolated compounds were assessed for their antimicrobial, antitubercular and cytotoxic activities. Among the tested compounds, the new labdane diterpenes **1**–**4** revealed significant cytotoxic activity against mouse lymphoma L5178Y cell line with IC_{50} values ranging from 1.4 to 12.9 µM, respectively.

Keywords: *Araucaria bidwillii*, labdane diterpene, antibacterial, cytotoxicity, TDDFT-ECD

1. Introduction:

Medicinal plants have been used in almost all cultures as a pivotal source of medicine for treatment and management of various human diseases. The traditional use of medicinal plants in developing countries, as a normative basis for the maintenance of good health, is widely observed. However, an increasing reliance on medicinal plants in the industrialized societies has been traced as well to develop several new drugs and chemotherapeutics in addition to the treatment of minor ailments.

Araucaria bidwillii is a plant belonging to family Araucariaceae with so diverse economical and agricultural uses in addition to be a traditional remedy for the treatment of amenorrhea (Aslam et al., 2013; Chen et al., 2011). The genus *Araucaria* has been distinguished by several reports in literature as a rich source of labdane diterpenes (Aslam et al., 2013; Chen et al., 2011; Noma et al., 1982; Caputo et al., 1976; Caputo et al., 1974) and bisflavonoids such as 7-*O*-methylcupressuflavone, 7,7"-di-*O*-methylagathisflavone, 7-*O*-methylagathisflavone, 4,7'"-di-*O*-methylagathisflavone and 7,7"di-*O*-methylcupressuflavone (Rahman et al., 1968). Labdane diterpenes are known to possess antialgal, antimicrobial and antiproliferative activities (Chen et al., 2011; Tanaka et al., 2000; Dimas et al., 1998; Jung et al., 1998).

In the current study, we report four new labdane diterpenoidal metabolites (**1**-**4**) (Figure 1) together with six known compounds including 7-oxocallitrisic acid (**5**) (Lee et al., 1994), two triterpenoidal metabolites namely, 2-*O*-acetyl-11-keto-boswellic acid (**6**) (Belsner et al., 2003; Csuk et al., 2015) and *β*-sitosterol-3-*O*-glucopyranoside (**7**) (Seo et al., 1978), in addition to phloretic acid (**8**) (Tanagornmeatar et al., 2014), two methylated bisflavonoids, agathisflavone-4',7,7"-trimethyl ether (**9**) (Ofman et al., 1995) and cupressuflavone-4',7,7"-trimethyl ether (**10**) (Inatomi et al., 2005; Ofman et al., 1995).

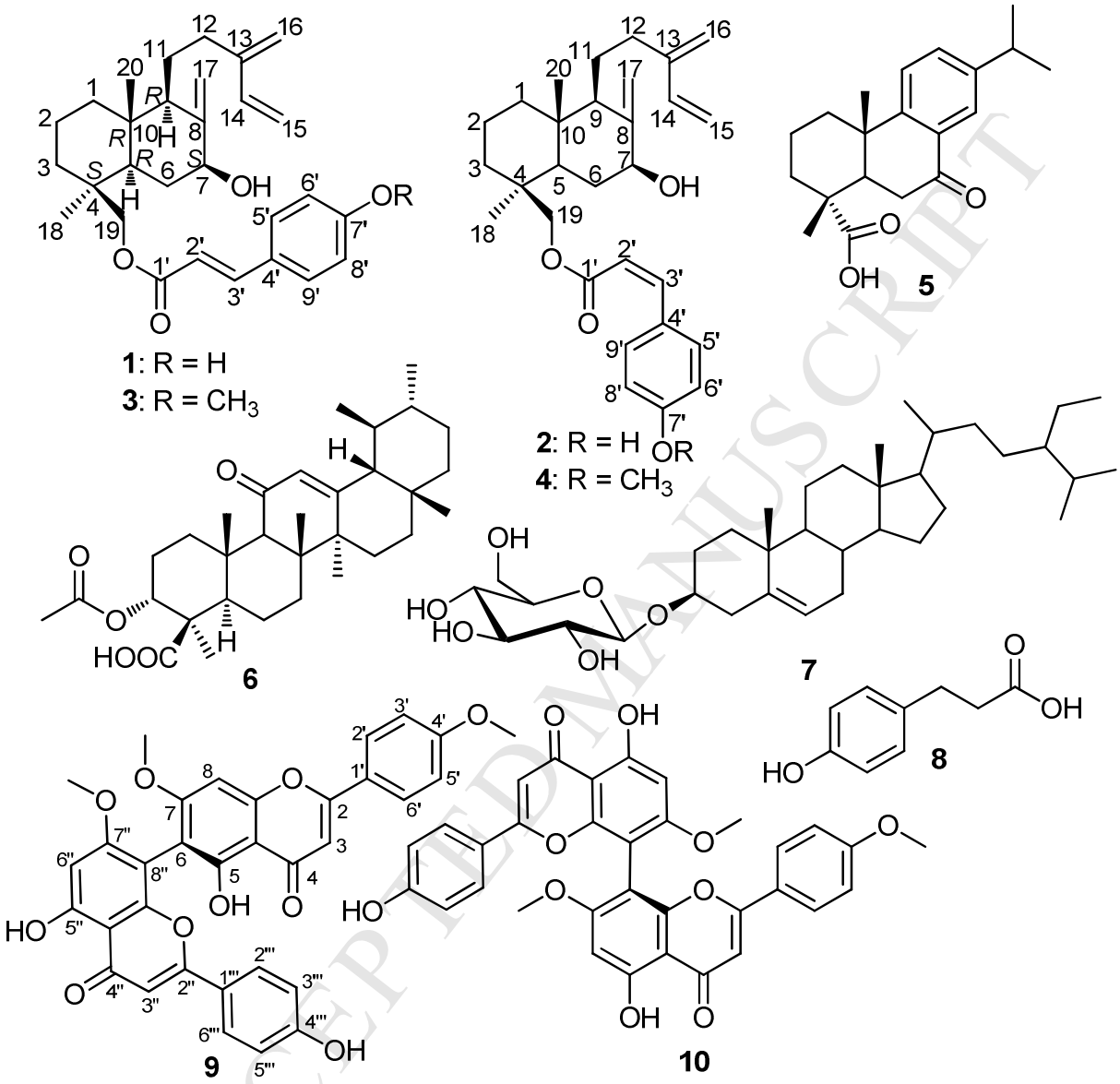

Figure 1. Chemical structures of the isolated compounds of *Araucaria bidwillii*

2. Results and Discussion

Compound **1** was isolated as an amorphous yellowish white solid. HRESIMS of **1** revealed a pseudomolecular ion peak at *m/z* 473.2662 $[M+Na]^+$ (calcd for 473.2668 $C_{29}H_{38}NaO_4$) indicating the existence of eleven degrees of unsaturation whereas its UV spectrum revealed absorption

maxima at 232 and 309 nm. ^{13}C NMR of **1** (Table 1) exhibited 29 different carbons divided into seven quaternary carbons including one carbonyl at δ_C 169.4; four olefinic quaternary carbons at δ_C 161.3, 151.4, 148.5 and 127.2 together with two aliphatic quaternary carbons at δ_C 40.0 and 38.5 ppm. Additionally, ^{13}C NMR spectrum of compound **1** showed 22 carbon resonances including aliphatic primary, secondary and tertiary carbons, olefinic tertiary and aromatic carbons. Based on ^{1}H and ^{13}C NMR of **1** (Table 1), compound **1** was suggested to be an ester derivative of labda-13(16),14-diene-19-ol diterpene as revealed by close similarity of its spectral data with labdane diterpenoidal esters isolated from *Juniperus thurifera* (San Feliciano et al., 1988) and *Chamaecyparis formosensis* (Lin et al., 1999). ^{1}H NMR, ^{1}H–^{1}H COSY and HMQC spectra of **1** (Table 1, see supplementary data) revealed proton resonances at δ_H 6.32 (1H, d, *J*= 16.0 Hz), 7.59 (1H, d, *J*= 16.0 Hz), 6.81 (2H, d, *J*= 8.7 Hz) and 7.47 (2H, d, *J*= 8.7 Hz) ppm ascribed for olefinic carbons at δ_C 115.2 (C-2'), 146.5 (C-3'), 116.8 (C-6' and C-8') and 131.2 (C5' and C-9') ppm, respectively, indicative for an (*E*)-*p*-hydroxycinnamoyl (= coumaroyl) moiety together with UV absorption maxima (λ_{max}) at 232 and 309 nm (Lin et al., 1999).

In addition, compound (**1**) displayed a hydroxy group at C-7 and an exocyclic methylene moiety at C-8 which was previously reported in labdane diterpenoids isolated from *A. cunninghamii* (Chen et al., 2011) and from *Nicotiana raimondii* (Noma et al, 1982). The exocyclic methylene moiety displayed proton resonances at δ_H 4.75 (1H, br s) and 5.27 (1H, br s) ppm which were correlated to the same carbon resonating at δ_C 104.1 ppm as shown through the HMQC experiment (see supplementary data). The position of the exocylic methylene moiety was unambiguously confirmed through further 2D NMR experiments such as HMBC (Figure 2a) which disclosed long range correlations with two tertiary aliphatic carbons at δ_C 74.8 and 55.0

assigned for C-7 and C-9, respectively, together with a correlation to an olefinic quaternary carbon at δ_C 151.4 ascribed to C-8.

Table 1. NMR Data of compounds (**1-4**).

#	**1**		**2**		**3**		**4**	
	δ_H[a] (multi, *J* value in Hz)	δ_C[b]	δ_H[a] (multi, *J* value in Hz)	δ_C[b]	δ_H[c] (multi, *J* value in Hz)	δ_C[d]	δ_H[e] (multi, *J* value in Hz)	δ_C[f]
1	1.07 (1H, m) 1.76 (1H, m)	39.9, CH_2	1.09 (1H, m) 1.77 (1H, m)	40.0, CH_2	1.00 (1H, m) 1.77 (1H, m)	38.9, CH_2	1.02 (1H, m) 1.72 (1H, m)	38.5, CH_2
2	0.88 (1H, m) 1.53 (1H, m)	20.0, CH_2	0.85 (1H, m) 1.52 (1H, m)	20.0, CH_2	1.52 (1H, m) 1.60 (1H, m)	19.1, CH_2	0.87 (1H, m) 1.52 (1H, m)	19.4, CH_2
3	1.12 (1H, m) 1.78 (1H, m)	37.7, CH_2	1.04 (1H, m) 1.67 (1H, m)	37.4, CH_2	1.06 (1H, m) 1.78 (1H, m)	36.7, CH_2	1.00 (1H, m) 1.52 (1H, m)	36.7, CH_2
4		38.5, C		38.3, C		37.6, C		36.4, C
5	1.63 (1H, m)	55.8, CH	1.60 (1H, m)	55.9, CH	1.60 (1H, m)	54.8, CH	1.56 (1H, m)	53.6, CH
6	1.39 (1H, m) 2.21 (1H, dd, 9.8, 5.2)	35.0, CH_2	1.34 (1H, m) 2.14 (1H, dd, 9.8, 5.2)	34.8, CH_2	1.37 (1H, m) 2.27 (1H, dd, 9.8, 5.2)	34.4, CH_2	1.28 (1H, m) 2.20 (1H, m)	34.1, CH_2
7	3.88 (1H, m)	74.8, CH	3.87 (1H, dd, 9.8, 5.2)	74.8, CH	3.96 (1H, dd, 9.8, 5.2)	74.3, CH	3.96 (1H, dd, 9.8, 5.2)	74.1, CH
8		151.4, C		151.4, C		150.1, C		154.6, C
9	1.39 (1H, m)	55.0, CH	1.32 (1H, m)	55.0, CH	1.33 (1H, m)	53.9, CH	1.28 (1H, m)	54.4, CH
10		40.0, C		40.0, C		39.3, C		38.9, C
11	1.63 (1H, m) 1.77 (1H, m)	23.4, CH_2	1.59 (1H, m) 1.69 (1H, m)	23.4, CH_2	1.60 (1H, m) 1.73 (1H, m)	22.2, CH_2	1.60 (1H, m) 1.73 (1H, m)	21.8, CH_2
12	2.05 (1H, m) 2.40 (1H, m)	31.0, CH_2	2.03 (1H, m) 2.37 (1H, m)	31.0, CH_2	2.00 (1H, m) 2.38 (1H, m)	30.0, CH_2	1.99 (1H, dd, 15.1, 9.1) 2.36 (1H, m)	30.0, CH_2
13		148.5, C		148.5, C		148.0, C		147.3, C
14	6.38 (1H, dd, 17.6, 11.0)	140.2, CH	6.39 (1H, dd, 17.6, 10.9)	140.2, CH	6.37 (1H, dd, 17.6, 11.0)	139.1, CH	6.36 (1H, dd, 17.6, 10.9)	139.7, CH
15	5.05 (1H, d, 11.0) 5.22 (1H, d, 17.6)	113.6, CH_2	5.06 (1H, d, 10.9) 5.23 (1H, d, 17.6)	113.6, CH_2	5.05 (1H, d, 11.0) 5.21 (1H, d, 17.6)	113.4, CH_2	5.05 (1H, d, 10.9) 5.20 (1H, d, 17.6)	113.2. CH_2
16	4.97 (1H, br s)	116.2,	4.98 (1H, br s)	116.1, CH_2	4.97 (1H, br s)	115.8, CH_2	4.96 (1H, br s)	115.6, CH_2

	5.00 (1H, br s)	CH_2	5.02 (1H, br s)		5.01 (1H, br s)		5.00 (1H, br s)	
17	4.75 (1H, br s) 5.27 (1H, br s)	104.1, CH_2	4.74 (1H, br s) 5.27 (1H, br s)	104.1, CH_2	4.97 (1H, br s) 5.23 (1H, br s)	103.5, CH_2	4.75 (1H, br s) 5.20 (1H, br s)	103.1, CH_2
18	1.07 (3H, s)	28.1, CH_3	0.98 (3H, s)	28.0, CH_3	1.06 (3H, s)	27.9, CH_3	0.96 (3H, s)	27.6, CH_3
19	3.99 (1H, d, 11.0) 4.38 (1H, d, 11.0)	67.9, CH_2	3.92 (1H, d, 11.0) 4.33 (1H, d, 11.0)	67.6, CH_2	3.96 (1H, d, 11.4) 4.36 (1H, d, 11.4)	66.8, CH_2	3.89 (1H, d, 11.2) 4.27 (1H, d, 11.2)	66.6, CH_2
20	0.73 (3H, s)	15.7, CH_3	0.74 (3H, s)	15.7, CH_3	0.72 (3H, s)	15.4, CH_3	0.69 (3H, s)	15.4, CH_3
1’		169.4, C		168.7, C		167.6, C		167.6, C
2’	6.32 (1H, d, 16.0)	115.2, CH	5.79 (1H, d, 12.7)	117.0, CH	6.29 (1H, d, 16.0)	115.9, CH	5.82 (1H, d, 12.7)	116.8, CH
3’	7.59 (1H, d, 16.0)	146.5, CH	6.88 (1H, d, 12.7)	144.6, CH	7.61 (1H, d, 16.0)	144.9, CH	6.84 (1H, d, 12.7)	143.2, CH
4’		127.2, C		127.3, C		127.3, C		127.6, C
5’,9’	7.47 (2H, d, 8.7)	131.2, CH	7.59 (2H, d, 8.7)	133.3, CH	7.48 (2H, d, 8.7)	130.0, CH	7.66 (2H, d, 8.7)	132.0, CH
6’,8’	6.81 (2H, d, 8.7)	116.8, CH	6.76 (2H, d, 8.7)	115.9, CH	6.90 (2H, d, 8.7)	114.5, CH	6.87 (2H, d, 8.7)	113.5, CH
7’		161.3, C		160.0, C		161.5, C		160.5, C
7’-OCH_3					3.84 (3H, s)	55.5, CH_3	3.82 (3H, s)	56.6, CH_3

[a] ^{1}H NMR measured in MeOH-d_4 at 600 MHz. [b] ^{13}C NMR measured in MeOH-d_4 at 150 MHz. [c] ^{1}H NMR measured in $CHCl_3$-d at 400 MHz. [d] ^{13}C NMR measured in $CHCl_3$-d at 100 MHz. [e] ^{1}H NMR measured in $CHCl_3$-d at 600 MHz. [f] ^{1}H NMR measured in $CHCl_3$-d at 150 MHz.

The hydroxyl group at C-7 revealed proton resonance at δ_H 3.88 (1H, m) and carbon resonance at δ_C 74.8 ppm as confirmed by HMQC experiment. The exact linkage of this hydroxyl group at C-7 was proven based upon HMBC experiments (Figure 2a) which revealed key long range correlations between the exocyclic methylene protons at δ_H 4.75 (1H, br s) and 5.27 (1H, br s) attached at C-8 and methylene protons at δ_H 1.39 (1H, m) and 2.21 (1H, dd, *J*= 9.8, 5.2 Hz) ppm assigned for C-6 to C-7 at δ_C 74.8 ppm. Moreover, a long range HMBC correlation was found between proton resonance at δ_H 3.88 (1H, m) at C-7 and carbon resonance at δ_C 35.0 ppm assigned for C-6. Based upon the aforementioned data, compound (**1**) was confirmed to be the new 7-hydroxy-labda-8(17),13(16),14-trien-19-yl-(*E*)-coumarate.

For establishing the relative and absolute configurations of **1**, a ROESY experiment (Figure 2b) and the modified Mosher's reaction (Table 2) were conducted, respectively. Results of Mosher's reactions of the hydroxyl group at C-7 unambiguously determined its absolute configuration as *S*, whereas the ROESY experiment (Figure 2b) revealed clear correlations between H-7 at δ_H 3.88 (1H, m) with two multiplet proton resonances at δ_H 1.39 and δ_H 1.63 ppm assigned for H-9 and H-5 in addition to a singlet methyl group at δ_H 1.07 ppm assigned for methyl group at C-4, respectively. ROESY experiment of **1** also revealed clear correlations between hydroxymethylene protons at δ_H 3.99 (1H, d, *J* = 11.0 Hz) and 4.38 (1H, d, *J* = 11.0 Hz) ppm, a singlet methyl group at δ_H 0.73 ppm and a methylene group at δ_H 1.63 (1H, m) and 1.77 (1H, m) ppm assigned for C-19, Me-20 and C-11, respectively. Based on the results obtained from Mosher's reaction and ROESY experiment, the absolute configuration of compound **1** was unambiguously determined to be 4*S*,5*R*,7*S*,9*R*,10*S* in accordance with the previously reported absolute configurations of chiral centers at C-5, C-9 and C-10 (Maldonado et al., 2015).

Table 2. Chemical shift differences between the (*S*)-MTPA and (*R*)-MTPA esters of compound (**1**).

position	Chemical shift (δ_H, in C_5D_5N, 600 MHz) in			Δ
	1	(*S*)-MTPA ester	(*R*)-MTPA ester	Δ(*S*) – δ(*R*)
6a	2.5435	2.5524	2.5379	+0.0145
6b	1.7721	1.8583	1.7144	+0.1439
17a	5.8916	5.7080	5.7304	-0.0224
17b	4.9525	4.6990	4.7082	-0.0092

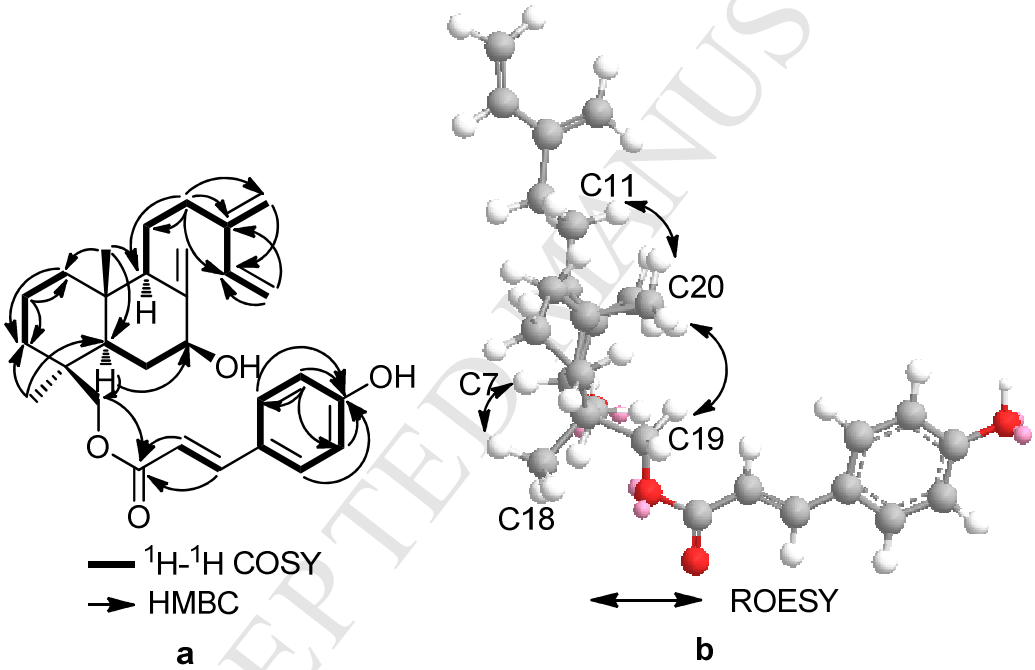

Figure 2. Key ^{1}H-^{1}H COSY, HMBC and ROESY correlations in compound (**1**).

Compound **2**, isolated as a yellowish white amorphous powder, revealed a pseudomolecular ion peak at *m/z* 473.2662 $[M+Na]^+$ (calcd for 473.2668 $C_{29}H_{38}NaO_4$) and UV absorption maxima (λ_{max}) at 231 and 307 nm similar to compound (**1**). In spite of the close similarity in spectral data of compounds **1** and **2** (Table 1), the latter displayed proton resonances

at δ_H 5.79 (1H, d, *J* = 12.7 Hz), 6.88 (1H, d, *J* = 12.7 Hz), 6.76 (2H, d, *J* = 8.7 Hz) and 7.59 (2H, d, *J* = 8.7 Hz) ppm attributable to (*Z*)-coumarate (Lin et al., 1999). The coupling constant of 12.7 Hz for the two olefinic protons in **2** was smaller than that in the *E*-isomer **1** where the coupling constant is 16.0 Hz. Apart from this difference between **1** and **2**, both revealed a close resemblance with regard to their 1D and 2D NMR spectral data including ^{1}H–^{1}H COSY, HMQC and HMBC experiments (Table 1, see supplementary data). Based on the biosynthetic relationship and having comparable optical rotation values, it was deduced that **1** and **2** share the same relative and absolute configurations which were supported by similar optical rotation values. In conclusion, compound **2** was unambiguously confirmed to be the new 7-hydroxy-labda-8(17),13(16),14-trien-19-yl-(*Z*)-coumarate which featured the absolute configuration 4*S*,5*R*,7*S*,9*R*,10*S*.

The molecular formula of compound **3** was established to be $C_{30}H_{40}O_4$ based on the existence of a pseudomolecular ion peak at *m/z* 482.3265 $[M+NH_4]^+$ (calcd for 482.3270 $C_{30}H_{44}NO_4$) indicating a difference of 14 amu compared to compounds **1** and **2**. ^{1}H NMR, ^{1}H–^{1}H COSY and HMQC spectra of **3** were similar to those of **1** (Table 1, see supplementary data) revealing proton resonances at δ_H 6.29 (1H, d, *J* = 16.0 Hz), 7.61 (1H, d, *J* = 16.0 Hz), 6.90 (2H, d, *J* = 8.7 Hz) and 7.48 (2H, d, *J* = 8.7 Hz) ppm ascribed for aromatic carbons at δ_C 115.9 (C-2'), 144.9 (C-3'), 114.5 (C-6' and C-8') and 130.0 (C5' and C-9') ppm, respectively, thus confirming the existence of an (*E*)-coumaroyl moiety in compound **3**. This was confirmed through the UV spectrum displaying maximal absorption peaks (λ_{max}) at 231 and 308 nm (Lin et al., 1999). ^{1}H and ^{13}C NMR spectral data of **3** (Table 1) disclosed that it comprises an additional singlet oxygenated methyl group at δ_H 3.84 ppm which was correlated to a primary oxygenated carbon resonance at δ_C 55.5 ppm as revealed by HMQC spectrum. In addition, HMBC spectrum of **3**

revealed a clear long range correlation between the methoxy group at δ_H 3.84 ppm and a quaternary aromatic carbon at δ_C 161.5 ppm indicating that the 14 amu difference is due to the methylation of phenolic hydroxyl group in the coumarate moiety. Apart from this difference, 1D and 2D NMR spectra including HMQC, HMBC and ROESY experiments of **3** closely resembled those of **1** in addition to **3** exhibiting a similar optical rotation value compared to that of **1**. Based on this close similarity in relative configuration and biosynthetic relationship between compounds **1** and **3**, the latter was unambiguously concluded to be 7-hydroxy-labda-8(17),13(16),14-trien-19-yl-7'-*O*-methyl-(*E*)-coumarate exhibiting probably the same absolute configuration 4*S*,5*R*,7*S*,9*R*,10*S* as elucidated for **1**.

The HRESIMS of compound **4** revealed pseudomolecular ion peaks at *m/z* 482.3265 $[M+NH_4]^+$ (calcd for 482.3270 $C_{30}H_{44}NO_4$) and 487.2819 $[M+Na]^+$ (calcd for 487.2824 $C_{30}H_{40}NaO_4$) indicating the molecular formula $C_{30}H_{40}O_4$ which is identical to that of **3.** ^{1}H NMR spectral data of **4** exhibited proton resonances similar to **2** in particular with regard to the two olefinic protons at δ_H 5.82 (1H, d, J = 12.7 Hz), 6.84 (1H, d, J = 12.7 Hz), 6.87 (2H, d, J = 8.7 Hz) and 7.66 (2H, d, J = 8.7 Hz) ppm which correlated to carbon resonances at δ_C 116.8 (C-2'), 143.2 (C-3'), 113.5 (C-6' and C-8') and 132.0 (C5' and C-9') ppm, respectively, as unambiguously disclosed by the HMQC experiment. In addition, the UV spectrum of **4** displayed absorption maxima (λ_{max}) at 232 and 305 nm which together with NMR spectral data indicated the presence of (*Z*)-coumarate moiety as a part of the structure (Lin et al., 1999). The coupling constant (*J* value) of 12.7 Hz for the two olefinic protons in **4** was smaller than that for the *E*-isomers **1** and **3** where the coupling constants amounted to 16.0 Hz. ^{1}H NMR spectral data of **4** (Table 1) revealed an additional singlet oxygenated methyl group at δ_H 3.82 ppm in comparison to **2** which was correlated to a primary oxygenated carbon resonance at δ_C 56.6 ppm as revealed

by the HMQC spectrum. In addition, the HMBC spectrum of **4** revealed a clear long range correlation between the methoxy group at δ_H 3.82 ppm and a quaternary aromatic carbon at δ_C 160.5 ppm indicating that the 14 amu difference is due to the methylation of phenolic hydroxyl group in the (*Z*)-coumarate moiety. Apart from this structural difference, 1D and 2D NMR spectra including HMQC, HMBC and ROESY experiments of **4** (Table 1, see supplementary data) closely resembled those of **2** in addition to similar optical rotation values that were observed for both compounds. Based on this close similarity in relative configuration and biosynthetic relationship compound **4** was unambiguously identified as 7-hydroxy-labda-8(17),13(16),14-trien-19-yl-7'-*O*-methyl-(*Z*)-coumarate for which the same absolute configuration 4*S*,5*R*,7*S*,9*R*,10*S* is proposed.

Compound **9** and **10** are heterodimeric biaryl natural products with 6,8'- and 8,8-linked flavone residues. Due to the substitution pattern and the position of the linkage, the biaryl systems of **9** and **10** have a high rotational energy barrier, which gives rise to atropisomerism (Bringmann et al., 2005). The specific rotation value and ECD spectra clearly indicated the presence of axial chirality, since both compounds contain no further chirality elements. The solution TDDFT-ECD calculation protocol has been efficiently utilized for the determination of axial chirality in biaryl natural products having hindered rotation (Rönsberg et al, 2013; Bara et al., 2013; Ola et al., 2014; Wu et al., 2015). Compound **9** is the 4',7,7"-trimethyl ether derivative of agathisflavone, the natural biaryl component of *Schinus terebinthifolius* Raddi (Anacardiaceae), the absolute configuration of which was studied by the combination of various chiroptical methods (ECD, VCD and ORD) and (*aS*) absolute configuration (positive $\omega_{C5\text{-}C6\text{-}C8''\text{-}C8a''}$ torsional angle) was assigned to the (–)-enantiomer (Covington et al., 2016). The ECD spectrum of compound **9** (Figure 3) had an oppositely signed pattern of Cotton effects (CEs)

compared to those of (–)-agathisflavone and an approximately 30 nm red shift of the corresponding CEs was also observed in acetonitrile.

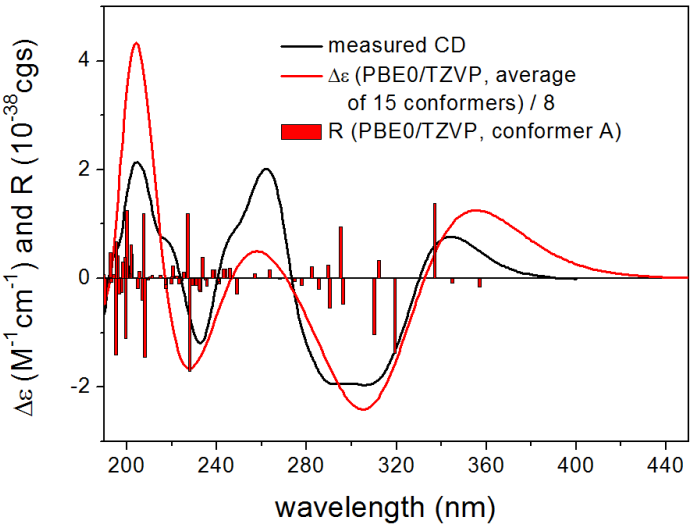

Figure 3. Experimental ECD spectrum of (+)-**9** in MeCN compared with the Boltzmann-weighted PBE0/TZVP ECD spectrum of (*aS*)-**9** computed for the B97D/TZVP PCM/MeCN conformers. Bars represent the rotational strength values of the lowest-energy conformer.

These data suggested that compound **9** had negative $\omega_{C5\text{-}C6\text{-}C8''\text{-}C8a''}$ torsional angle, opposite to that of (–)-agathisflavone, which however is also denoted by (*aS*) axial chirality, since the different substitution pattern alters the priority order. In order to test the applicability of our solution TDDFT-ECD protocol for biaryl natural products on the axial chirality of **9** and confirm its absolute configuration, ECD calculations of **9** were carried out (Pescitelli and Bruhn, 2016; Mándi et al., 2015). MMFF conformational search resulted in 136 conformers [with (*aR*) and (*aS*) axial chirality] in a 21 kJ/mol energy window. Conformers with negative $\omega_{C5\text{-}C6\text{-}C8''\text{-}C8a''}$ torsional angles [(a*S*) axial chirality] (Figure 4) were selected and reoptimized at the B3LYP/6-

31G(d) in vacuo and the B97D/TZVP (Grimme, 2006; Sun et al., 2013) PCM/MeCN levels of theory.

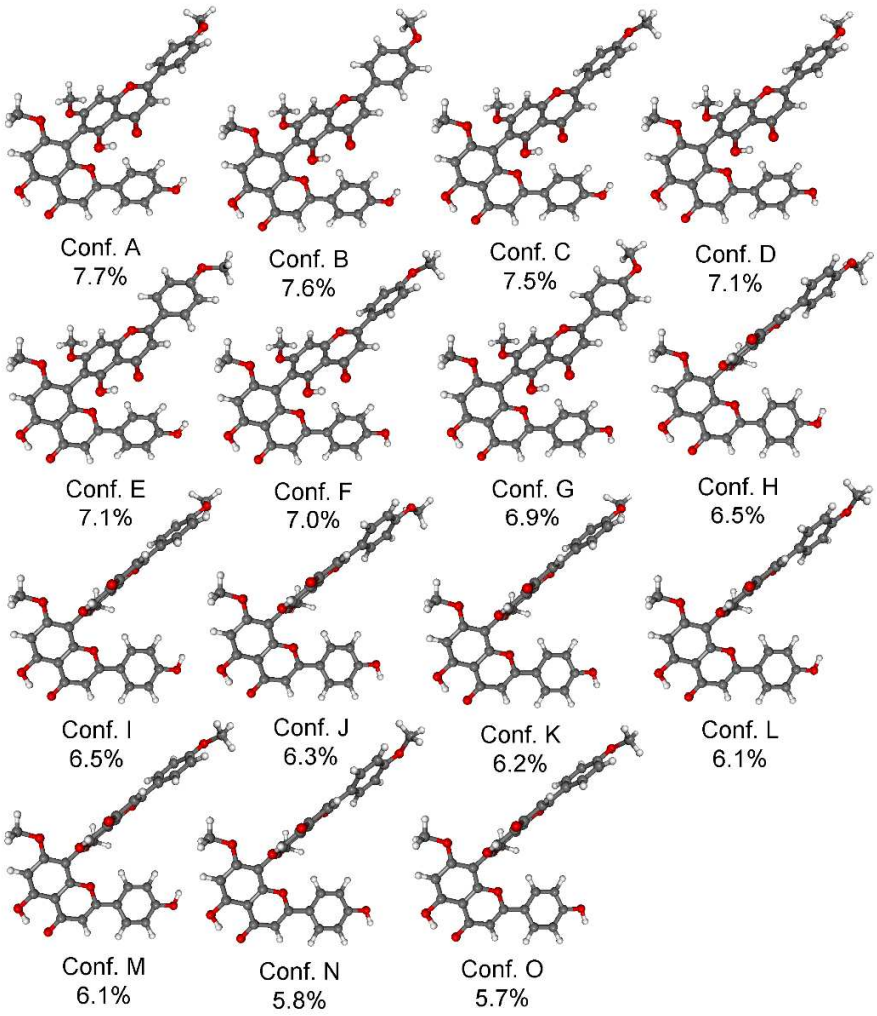

Figure 4. Structures and populations of the low-energy B97D/TZVP PCM/MeCN conformers (≥1%) of (*aS*)-**9**.

ECD spectra computed for the low-energy (≥ 1%) conformers at various levels gave moderate to good agreement with the experimental spectrum of **9** allowing elucidation of the absolute configuration as (*aS*). By analyzing the compouted ECD spectra of the individual conformers, it turned out that the 340 and 260 nm ECD transitions are sensitive to both the biaryl

and the flavone ($\omega_{C3,C2,C1',C2'}$) torsional angles. For the (*aS*) enantiomer, the low-energy conformers of **9** have an $\omega_{C5\text{-}C6\text{-}C8''\text{-}C8a''}$ torsional angle of either ca. –67° or ca. –107° (B97D/TZVP PCM/MeCN values). Furthermore, among the low-energy conformers, there were geometries with both positive and negative $\omega_{C3,C2,C1',C2'}$ flavone torsional angles, which resulted in inversion of 340 and 260 nm CE (conformers E and H in Figure 5). Since substitution pattern of related molecules can alter both torsional angles, these transitions are not recommended for comparison to elucidate absolute configuration of agathisflavone derivatives when simple ECD correlation is applied. (–)-Agathisflavone and (+)-**9** represent an example for chiral switching (Ebrahim et al., 2012; Zhang et al., 2015) of natural products when related natural derivatives are produced with opposite absolute configuration in different organisms.

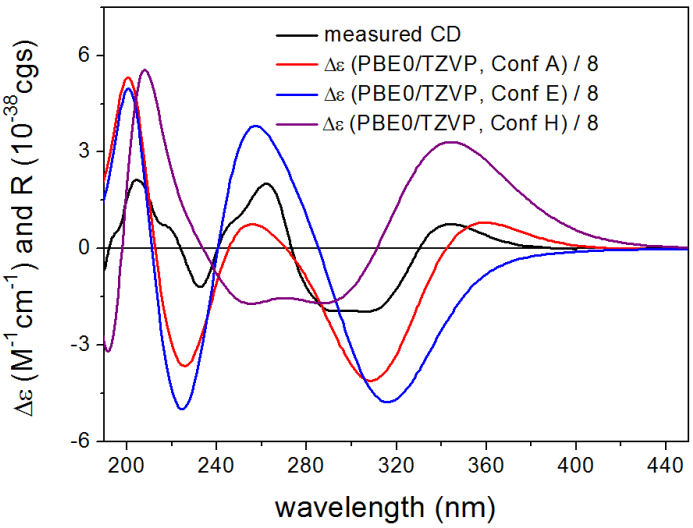

Figure 5. Experimental ECD spectrum of **9** in MeCN compared with the PBE0/TZVP ECD spectrum of conformers A, E and H of (*aS*)-**9**. Level of optimization: B97D/TZVP PCM/MeCN

Compound **10**, the 8,8'-linked heterodimeric flavone biaryl derivative, had positive CE at 357 nm and negative one at 322 nm in the ECD spectrum, which allowed the assignment of axial chirality as (a*R*) on the basis of the ECD spectrum of the related cupressuflavone 4'-O-β-D-glucopyranosides (Inatomi et al., 2005).

All isolated compounds were assessed for their antiproliferative activity(ies) against the mouse lymphoma (L5178Y) cell line using the *in vitro* cytotoxicity (MTT) assay and kahalalide F as a standard antiproliferative agent. Results (Table 3) revealed that among the four new labdane derivatives (**1**–**4**), compounds **1** and **2** revealed IC_{50} values of 2.22 and 1.42 µM, respectively. Both compounds are thus more potent than the standard drug kahalalide F with an IC_{50} value of 4.30 µM.

Table 3. Cytotoxic activity of isolated compounds against mouse lymphoma L5178Y cell line.

Compound	L5178Y % Growth inhibition (10 µg/mL)	EC_{50} in µM
1	100	2.22
2	100	1.42
3	65	n.a.
4	22	12.9
5	94	>30
Kahalalide F		4.30

n.a.: not active.

However, their respective methylated derivatives (**3** and **4**) exhibited moderate to no activity. These results suggest preliminary structure activity relationships (SAR) such as i) the configuration of the olefinic double bond of coumarate moiety does not significantly affect the cytotoxicity, ii) although methylation of the phenolic hydroxyl group does increase the lipophilicity which in turn increases its cellular uptake and bioactivity, compounds (**3** and **4**)

showed moderate or no activity compared to the non-methylated metabolites (**1** and **2**) presumably being due to steric hindrance leading to decreased binding to the yet unknown target receptors.

Experimental section

2.1. General experimental procedures

Optical rotation was determined using a Perkin-Elmer-241 MC polarimeter. Mass spectrometry was measured on a LC-MS HP1100 Agilent Finnigan LCQ Deca XP Thermoquest whereas high-resolution mass spectra (HRESIMS) were recorded on FTHRMS-Orbitrap (Thermo Finnigan) mass spectrometer. Analytical HPLC measurements were conducted on Dionex Ultimate 3000 LC system coupled with a photodiode array detector (UVD340S), using detection channels at 235, 254, 280 and 340 nm wavelengths. Ready-made separation columns (125 × 4 mm, L × ID), prefilled with Eurospher-10C_{18} (Knauer, Germany), were used implementing a gradient elution as follows, (MeOH, 0.01% HCOOH in H_2O): 0 min, 10% MeOH; 5 min, 10% MeOH; 35 min, 100% MeOH; 45 min, 100% MeOH, with a flow rate of 1 mL/min. Preparative HPLC separation was accomplished using a RP-HPLC system of LaChrom-Merk Hitachi (pump: L7100 and UV detector L7400; column: Eurospher 100C_{18}, 300 × 8 mm, Knauer, Germany) with a flow rate of 5.0 mL/min. Routine normal phase column chromatography was performed using Merck MN silica gel 60 M (0.04-0.063 mm) or Sephadex LH-20 as stationary phases. 1D (^{1}H and ^{13}C NMR) and 2D NMR (chemical shifts in ppm) spectra were measured by Bruker AVANCE DMX 600 and AVANCE HD III 400 MHz NMR spectrometer (Switzerland) using methanol-d_4 and chloroform-*d* solvents (Sigma Aldrich, Germany). ECD spectra were recorded on a J-810 spectropolarimeter. Ready-made TLC plates precoated with silica gel 60 F_{254} (Merck, Darmstadt, Germany) were used for analytical purposes followed by detection under UV light at 254 and

365 nm wavelengths or after spraying with anisaldehyde and vanillin sulfuric acid spray reagents. Solvents used during the experiments were distilled before being used. Spectroscopic and deuterated grade solvents were used for spectroscopic and NMR measurements, respectively.

2.2. Plant material

Fresh leaves (7 kg) of *A. bidwillii* were collected at the Zoo Garden, Giza, Egypt, in January 2015 and authenticated by Mrs. Therease Labib, consultant at Orman Botanical Garden and National Gene Bank, Giza, Egypt. A voucher specimen was deposited at Department of Pharmacognosy, Faculty of Pharmacy, Ain-Shams University given a code PHG-P-AB192.

2.3. Extraction, isolation and purification

Air-dried grounded leaves were extracted with methanol then evaporated till dryness yielding a solid residue of 313 g which was subjected to liquid-liquid fractionation between its aqueous dispersion (1.0 L) and petroleum ether (Pet. Ether, 3.0 L), ethyl acetate (EtOAc, 8.0 L), and butanol (*n*-BuOH, 8.0 L), each at room temperature to afford different fractions weighing 0.71, 21.0 g and 56.0 g, respectively. From EtOAc extract about 10 g were fractionated over an open column packed with silica gel (250 g) as adsorbent. The elution process started with petroleum ether and then ethyl acetate was added gradually to increase the polarity of the eluent till reaching 100% ethyl acetate. Next dichloromethane and methanol in different ratios till reaching 100% methanol were used to elute the column. Finally, the column was washed with acetone (100%). The elution process was inspected under UV light. Thirty fractions (500 mL each) were collected and monitored by TLC on silica gel plates. The TLC was examined under UV light and sprayed with vanillin sulphuric reagent. Similar fractions were pooled together and dried to give 24 subfractions (A–X).

Fraction D (330 mg) eluted by Pet. Ether:EtOAc (8:2) was further purified by preparative HPLC resulting in the isolation and identification of compounds **3** (0.7 mg) and **4** (1.0 mg). Fraction F (350 mg) eluted with Pet. Ether:EtOAc (8:2) was further purified by preparative HPLC resulting in the isolation and identification of compounds **1** (6.6 mg) and **2** (6.9 mg), whereas fraction G (240 mg) eluted by Pet. Ether:EtOAc (3:2) was subjected to preparative HPLC for further purification yielding compounds **5** (2.8 mg) and **6** (5.6 mg). Fractions I and J (390 mg) also eluted by Pet. Ether:EtOAc (3:2) were also purified using preparative HPLC yielding compounds **8** (6.1 mg), **9** (2.3 mg) and **10** (8.3 mg). Fraction N (300 mg) eluted by 100% EtOAc yielded compound **7** (1.2 mg) by crystallization.

2.3.1. *7-Hydroxy-labda-8(17),13(16),14-trien-19-yl-(E)-coumarate (**1**)*. Yellowish white solid; $[\alpha]_D^{20}$ +4.0 (*c* 0.70, MeOH); UV (MeOH) λ_{max}: 232 and 309 nm; ^{1}H and ^{13}C NNR data see Table 1; HRESIMS $[M+Na]^+$ *m/z* 473.2662 (calcd for 473.2668 $C_{29}H_{38}NaO_4$).

2.3.2. *7-Hydroxy-labda-8(17),13(16),14-trien-19-yl-(Z)-coumarate (**2**)*. Yellowish white amorphous powder; $[\alpha]_D^{20}$ +17.5 (*c* 0.70, MeOH); UV (MeOH) λ_{max}: 231 and 307 nm; ^{1}H and ^{13}C NNR data see Table 1; HRESIMS $[M+Na]^+$ *m/z* 473.2662 (calcd for 473.2668 $C_{29}H_{38}NaO_4$).

2.3.3. *7-Hydroxy-labda-8(17),13(16),14-trien-19-yl-7'-O-methyl-(E)-coumarate (**3**)*. Amorphous off-white solid; $[\alpha]_D^{20}$ +7.5 (*c* 0.70, MeOH); UV (MeOH) λ_{max}: 231 and 308 nm; ^{1}H and ^{13}C NNR data see Table 1; HRESIMS $[M+NH_4]^+$ *m/z* 482.3265 (calcd for 482.3270 $C_{30}H_{44}NO_4$).

2.3.4. *7-Hydroxy-labda-8(17),13(16),14-trien-19-yl-7'-O-methyl-(Z)-coumarate (**4**)*. Off-white amorphous powder; $[\alpha]_D^{20}$ +25.5 (*c* 0.70, MeOH); UV (MeOH) λ_{max}: 232 and 305 nm; ^{1}H and ^{13}C NNR data see Table 1; HRESIMS $[M+NH_4]^+$ *m/z* 482.3265 (calcd for 482.3270 $C_{30}H_{44}NO_4$) and $[M+Na]^+$ *m/z* 487.2819 (calcd for 487.2824 $C_{30}H_{40}NaO_4$).

2.3.5. *Agathisflavone-4',7,7"-trimethyl ether (**9**)*. Yellow amorphous powder; $[\alpha]_D^{20}$ +33.0 (*c* 0.60, MeOH); UV (MeOH) λ_{max}: 206, 220, 272 and 328 nm; ECD (MeCN, λ [nm] (Δε), c 0.172 mM): 344 (+0.76), 306 (-1.96), 292 (-1.94), 262 (+2.01), 246sh (+0.77), 233 (–1.19), 217sh (+0.72), 205 (+2.13); ^{1}H NMR data (Ofman et al., 1995); HRESIMS $[M+H]^+$ *m/z* 581.1442 (calcd for 581.1448 $C_{33}H_{25}NO_{10}$).

2.3.6. *Cupressuflavone-4',7,7"-trimethyl ether (**10**)*. Yellow amorphous powder; $[\alpha]_D^{20}$ -63.4 (*c* 0.30, MeOH); UV (MeOH) λ_{max}: 206, 225, 272 and 340 nm; ECD (MeCN, λ [nm] (Δε), c 0.172 mM): 357 (+4.07), 322 (-9.55), 305sh (-4.45), 267 (+3.60), 243 (+0.62), 226 (+1.58), 215 (-0.37), 207 (+2.11); ^{1}H NNR data (Inatomi et al., 2005; Ofman et al., 1995); HRESIMS $[M+H]^+$ *m/z* 581.1442 (calcd for 581.1448 $C_{33}H_{25}NO_{10}$).

2.4. Mosher's reaction

Chiral derivatization was conducted following the convenient Mosher ester method as previously described in the literature (Su et al., 2002). The tested compounds (2 × 1 mg each) were transferred into clean dry NMR tubes under a N_2 gas stream. The samples (1 mg) were dissolved in deuterated pyridine (0.5 mL), and both (*R*)- and (*S*)-*α*-methoxy-*α*-(trifluoromethyl)phenylacetic (MTPA) acid chloride were added separately into the NMR tubes, immediately under a N_2 gas stream. The reagent was added in the ration of 0.14 mM reagent to 0.10 mM of the compound (Dale and Mosher, 1973). Careful shaking of the NMR tubes was performed to assure thorough mixing of the samples and MTPA chloride. The reaction NMR tubes were kept at room temperature and monitored by ^{1}H NMR spectroscopy until the reaction was complete. ^{1}H–^{1}H COSY spectra were measured to confirm the assignment of the signals.

2.5. Cytotoxicity (MTT) assay

Antiproliferative activity was assessed against mouse lymphoma (L5178Y) cell line, using a microplate 3-(4,5-dimethythiazole-2yl)-2,5-diphenyl-tetrazolium bromide (MTT) assay as previously described (Ashour et al., 2006). All experiments were carried out in triplicate and repeated thrice. The cytotoxic depsipeptide kahalalide F (IC_{50} = 4.3 µM) was used as a positive control and a medium containing 0.1% EGMME-DMSO was used as a negative control.

2.6. Computational Section

Mixed torsional/low mode conformational searches were carried out by means of the Macromodel 9.9.223 (MarcoModel, 2012) software using Merck Molecular Force Field (MMFF) with implicit solvent model for $CHCl_3$ applying a 21 kJ/mol energy window. Geometry optimizations [B3LYP/6-31G(d) in vacuo and B97D/TZVP (Grimme, 2006; Sun et al., 2013) with PCM solvent model for MeCN] and TDDFT calculations were performed with Gaussian 09 using various functionals (B3LYP, BH&HLYP and PBE0) and TZVP basis set (Frisch et al., 2010). ECD spectra were generated as the sum of Gaussians with 3000 cm^{-1} half-height width (corresponding to c.a. 20 nm at 260 nm), using dipole-velocity computed rotational strengths (Stephens and Harada, 2010). Boltzmann distributions were estimated from the ZPVE-corrected B3LYP/6-31G(d) energies in the gas-phase calculations and from the B97D/TZVP energies in the solvated ones. The MOLEKEL software package was used for visualization of the results (Marcomodel, 2012).

Acknowledgements

P.P. wants to thank Manchot Foundation for support. The research of the Hungarian authors was supported by the EU and co-financed by the European Regional Development Fund under the project GINOP-2.3.2-15-2016-00008. We thank the Governmental Information-Technology Development Agency (KIFÜ) for CPU time.

Supplementary data

References and notes

Ashour, M.; Edrada-Ebel, R. A.; Ebel, R.; Wray, V.; Wätjen, W.; Padmakumar, K.; Müller, W. E. G.; Lin, W. H.; Proksch, P. *J. Nat. Prod.* **2006**, *69*, 1547-1553.

Aslam, M. S.; Choudhary, B. A.; Uzair, M.; Ijaz, A. S. *Trop. J. Pharm. Res.* **2013**, *12*, 651-659.

Bara, R.; Zerfass, I.; Aly, A. H.; Goldbach-Gecke, H.; Raghavan, V.; Sass, P.; Mándi, A.; Wray, V.; Polavarapu, P. L.; Pretsch, A.; Lin, W. H.; Kurtán, T.; Debbab, A.; Brötz-Oesterhelt, H.; Proksch, P. *J. Med. Chem.* **2013**, *56*, 3257-3272.

Belsner, K.; Büchele, B.; Werz, U.; Syrovets, T.; Simmet, T. *Magn. Reson. Chem.* **2003**, *41*, 115-122.

Bringmann, G.; Price Mortimer, A. J.; Keller, P. A.; Gresser, M. J.; Garner, J.; Breuning, M. *Angew. Chem. Int. Ed.* **2005**, *44*, 5384-5427.

Caputo, R.; Dovinola, V.; Mangoni, L. *Phytochemistry* **1974**, *13*, 475-478.

Caputo, R.; Mangoni, L.; Monaco, P.; Pelosi, L.; Previtera, L. *Phytochemistry* **1976**, *15*, 1401-1402.

Chen, J.; Chen, J.-J.; Yang, L.-Q.; Hua, L.; Gao, K. *Planta Med.* **2011**, *77*, 485-488.

Covington, C. L.; Junior, F. M. S.; Silva, J. H. S.; Kuster, R. M.; de Amorim, M. B.; Polavarapu, P. L. *J. Nat. Prod.* **2016**, *79*, 2530-2537.

Csuk, R.; Barthel-Niesen, A.; Barthel, A.; Schäfer, R.; Al-Harrasi, A. *Eur. J. Med. Chem.* **2015**, *100*, 98-105.

Dale, J. A.; Mosher, H. S. *J. Am. Chem. Soc.* **1973**, *95*, 512-519.

Dimas, K.; Demetzos, C.; Marsellos, M.; Sotiriadou, R.; Malamas, M., Kokkinopoulos, D. *Planta Med.* **1998**, *64*, 208-211.

Ebrahim, W.; Aly, A. H.; Mándi, A.; Totzke, F.; Kubbutat, M. H. G.; Wray, V.; Lin, W.; Dai, H.; Proksch, P.; Kurtán, T.; Debbab, A. *Eur. J. Org. Chem.* **2012**, 3476-3484.

Ebrahim, W.; El-Neketi, M.; Lewald, L.-I.; Orfali, R. S.; Lin, W. H.; Rehberg, N.; Kalscheuer, R.; Daletos, G.; Proksch, P. *J. Nat. Prod.* **2016**, *79*, 914-922.

Frisch, M. J.; Trucks, G. W.; Schlegel, H. B.; Scuseria, G. E.; Robb, M. A.; Cheeseman, J. R.; Scalmani, G.; Barone, V.; Mennucci, B.; Petersson, G. A.; Nakatsuji, H.; Caricato, M.; Li, X.; Hratchian, H. P.; Izmaylov, A. F.; Bloino, J.; Zheng, G.; Sonnenberg, J. L.; Hada, M.; Ehara, M.; Toyota, K.; Fukuda, R.; Hasegawa, J.; Ishida, M.; Nakajima, T.; Honda, Y.; Kitao, O.; Nakai, H.; Vreven, T.; Montgomery, J. A., Jr.; Peralta, J. E.; Ogliaro, F.; Bearpark, M.; Heyd, J. J.; Brothers, E.; Kudin, K. N.; Staroverov, V. N.; Kobayashi, R.; Normand, J.; Raghavachari, K.; Rendell, A.; Burant, J. C.; Iyengar, S. S.; Tomasi, J.; Cossi, M.; Rega, N.; Millam, J. M.; Klene, M.; Knox, J. E.; Cross, J. B.; Bakken, V.; Adamo, C.; Jaramillo, J.; Gomperts, R.; Stratmann, R. E.; Yazyev, O.; Austin, A. J.; Cammi, R.; Pomelli, C.; Ochterski, J. W.; Martin, R. L.; Morokuma, K.; Zakrzewski, V. G.; Voth, G. A.; Salvador, P.; Dannenberg, J. J.; Dapprich, S.; Daniels, A. D.; Farkas, Ö.; Foresman, J. B.; Ortiz, J. V.; Cioslowski, J.; Fox, D. J. Gaussian 09, revision B.01; Gaussian, Inc.: Wallingford, CT, 2010.

Grimme, S. *J. Comput. Chem.* **2006**, *27*, 1787-1799.

Inatomi, Y.; Iida, N.; Murata, H.; Inada, A.; Murata, J.; Lang, F. A.; Iinuma, M.; Tanaka, T.; Nakanishi, T. *Tetrahedron Lett.* **2005**, *46*, 6533-6535.

Jung, M.; Ko, I.; Lee, S.; Choi, S. J.; Youn, B. H.; Kim, S. K. *Bioorg. Med. Chem. Lett.* **1998**, *8*, 3295-3298.

Lee, C.-K.; Fang, J.-M.; Cheng, Y.-S. *Phytochemistry* **1994**, *35*, 983-986.

Lin, T.-C.; Fang, J.-M.; Cheng, Y.-S. *Phytochemistry* **1999**, *51*, 793-801.

MacroModel; Schrödinger, LLC, 2012, http://www.schrodinger.com/MacroModel

Maldonado, E.; Pérez-Castorena, A. L.; Romero, Y.; Martínez, Mahinda. *J. Nat. Prod.* **2015**, *78*, 202-207.

Mándi, A.; Mudianta, I. W.; Kurtán, T.; Garson, M. J. *J. Nat. Prod.* **2015**, *78*, 2051-2056.

Noma, M.; Suzuki, F.; Gamou, K.; Kawashima, N. *Phytochemistry* **1982**, *21*, 395-397.

Ofman, D. J.; Markham, K. R.; Vilain, C.; Molloy, B. P. J. *Phytochemistry* **1995**, *38*, 1223-1228.

Ola, A. R. B.; Debbab, A.; Aly, A. H.; Mándi, A.; Zerfass, I.; Hamacher, A.; Kassack, M. U.; Brötz-Oesterhelt, H.; Kurtán, T.; Proksch, P. *Tetrahedron Lett.* **2014**, *55*, 1020-1023.

Pescitelli, G.; Bruhn, T. *Chirality* **2016**, *28*, 466-474.

Rahman, W.; Bhatnagar, S. P. *Tetrahedron Lett.* **1968**, *6*, 675-678.

Rönsberg, D.; Debbab, A.; Mándi, A.; Vasylyeva, V.; Böhler, P.; Stork, B.; Engelke, L.; Hamacher, A.; Sawadogo, R.; Diederich, M.; Wray, V.; Lin, W. H.; Kassack, M. U.; Janiak, C.; Scheu, S.; Wesselborg, S.; Kurtán, T.; Aly, A. H.; Proksch, P. *J. Org. Chem.* **2013**, *78*, 12409-12425.

San Feliciano, A.; Medarde, M.; Lopez, J. L.; Miguel del Corral, J. M.; Puebla, P.; Barrero, A. F. *Phytochemistry* **1988**, *27*, 2241-2248.

Seo, S.; Tomita, Y.; Tori, K.; Yoshimura, Y. *J. Am. Chem. Soc.* **1978**, *100*, 3331-3339.

Stephens, P. J.; Harada, N., ECD cotton effect approximated by the Gaussian curve and other methods. *Chirality* **2010**, *22*, 229-233.

Su, B.-N.; Park, E. J.; Mbwambo, Z. H.; Santarsiero, B. D.; Mesecar, A. D.; Fong, H. H. S.; Pezzuto, J. M.; Kinghorn, A. D. *J. Nat. Prod.* **2002**, *65*, 1278-1282.

Sun, P.; Xu, D. X.; Mándi, A.; Kurtán, T.; Li, T. J.; Schulz, B.; Zhang, W. *J. Org. Chem.* **2013**, *78*, 7030-7047.

Tanaka, R.; Ohtsu, H.; Iwamoto, M.; Minami, T.; Tokuda, H.; Nishino, H. *Cancer Lett.* **2000**, *161*, 165-170.

Tanagornmeatar, K.; Chaotham, C.; Sritularak, B.; Likhitwitayawuid, K.; Chanvorachote, P. *Anticancer Res.* **2014**, *34*, 6573-6580.

Varetto, U. MOLEKEL, v. 5.4; Swiss National Supercomputing Centre: Manno, Switzerland, 2009.

Wu, G.; Yu, G.; Kurtán, T.; Mándi, A.; Peng, J.; Mo, X.; Liu, M.; Li, H.; Sun, X.; Li, J.; Zhu, T.; Gu, Q.; Li, D. *J. Nat. Prod.* **2015**, *78*, 2691-2698.

Zhang, P.; Meng, L.-H.; Mándi, A.; Li, X.-M.; Kurtán, T.; Wang, B.-G. *RSC Adv.* **2015**, *5*, 39870-39877.